Exploiting MIMO in the Personal Sphere

Dries Neirynck, Chris Williams, Andrew Nix and Mark Beach

Centre for Communications Research, University of Bristol

Merchant Venturers Building, Woodland Road, BS8 1UB, Bristol, UK

Email: d.neirynck@tue.nl, m.a.beach@bristol.ac.uk

Abstract

This paper presents an analysis of the propagation characteristics of communication links in the personal sphere. The results of two wideband measurement campaigns in the 5.2 GHz band involving on-body MIMO arrays are reported.

In the first measurement, transmission takes place between on-body antennas and a uniform linear array, positioned at close range and with line-of-sight propagation conditions. Despite the LOS operation, MIMO is shown to offer a significant increase in the information theoretic capacity of the system when compared with a conventional SISO antenna system. Although this appears counter-intuitive to the well-known fact that uncorrelated scattering results in high capacity, two previously less well-known mechanisms are highlighted to explain this result. This analysis reveals the potential use of MIMO in personal area networks.

The second measurement campaign uses two on-body MIMO arrays to focus on the subject of body area network propagation. Analysis of the SISO characteristics of the links highlights the influence of the user on the channel. Body shadowing and user motion are shown to lead to multiple rapid changes in the channel characteristics. Again, MIMO is shown to be able to offer performance enhancement. In the measured channels, polarisation diversity is shown to outperform spatial diversity.

I. Introduction

The potential of multiple-input, multiple-output (MIMO) antenna systems to increase the capacity of a wireless link is well-known [1]. Its use in cellular and WLAN applications has been extensively studied [2], [3], [4]. Through theoretical analysis and measurements, fading correlation [5], [6] and power imbalances [3] were shown to have a negative influence on MIMO performance.

In the personal sphere, the concept of personal area networks (PAN) has driven the development of technologies such as Bluetooth and IEEE 802.15.3. Whereas Bluetooth [7] was originally intended as a cheap cable replacement technology, newer standards are being developed with ever-increasing data rates in mind [8], [9]. To date, the use of MIMO for PAN applications has not been considered. It is generally assumed that the high probability of a line-of-sight (LOS), and the subsequent correlation between the subchannels, prevents MIMO from offering throughput benefits in a PAN environment. This scepticism towards MIMO for PAN applications is reflected in the lack of available literature in this area. To the authors' knowledge, only the IST-MAGNET project has published a description of a MIMO measurement campaign using PAN devices [10]. However, the reported analysis is almost entirely restricted to single-input, single output (SISO) channel characteristics.

In this paper, two novel measurement campaigns in the personal sphere are described. The results highlight the influence of the user on the channel characteristics and dispel the common view that MIMO based antenna signal processing has no

Dries Neirynck is currently with the Radiocommunications Group at Eindhoven University of Technology.

benefit in PAN applications.

In the first measurement campaign, it is observed that the MIMO theoretic information capacity of a LOS link over a 1 metre distance exceeds that of the independent, identically distributed (IID) Rayleigh fading reference channel. This result is explained using a combination of previously less-known and more recent theoretical knowledge. A new sensitivity analysis is also performed to explain how the MIMO results still apply despite a 10 dB power imbalance due to body mounting of the antennas.

The second measurement campaign focuses on communication between two on-body locations. The term body area network (BAN) is used to distinguish this case from scenarios where only one of the devices is carried by the user. In these measurements, MIMO also offers a significant capacity increase compared to SISO. Despite the short range, LOS is far less common than expected. Moreover, misalignment of directional antennas, which are necessary to reduce the amount of radiation exposed to the user, means that the LOS component is often not dominant.

Next generation systems will be far more user-centric. Therefore, it can be expected that PAN will be a core element of 4G architectures. The results presented in this paper imply that MIMO should be considered as a candidate for next-generation PAN air interfaces. The presence of the multiple antennas could be exploited to mirror the high capacity of the bearer networks or, in combination with space-time coding, to save transmit power or to reduce the probability of link failure due to body shadowing.

The remainder of this paper is organised as follows. Section II describes the first measurement campaign. Subsections contain the results and analysis of the SISO and MIMO channel characterisation. Section III respects this structure for the BAN measurements. Concluding remarks are given in section IV.

II. LOS MIMO Operation in a PAN

A. Measurement description

A person equipped with two on-body antennas was placed in a standing position at short distances from a linear array. Using a Medav RUSK channel sounder [11], the MIMO channels between the user and the array were recorded using a 120 MHz measurement bandwidth centred at 5.2 GHz. The experiment was conducted with the person standing at 1, 2 and 3 metres from the linear array.

Because of consumer concerns and legal requirements, it is expected that on-body antennas will be directional to ensure that RF energy flows away from the user. Dual-polar stacked patch antennas were chosen since they fit this criterion. The design and characteristics of the antennas used is discussed in [12]. For this experiment, the antennas were mounted at chest height on top of the user's clothing and were spaced 15 centimetres apart. Table I gives a summary of the measured on-body characteristics.

A uniform linear array was used at the receiving end. The array consists of eight cavity backed dipoles spaced at half wavelength intervals. Additional passive elements were also included on the array in order to reduce mutual coupling effects. During the measurement period, the linear array was placed at a height of 120 centimetres on a trolley containing the channel sounder.

The measurements were performed in a medium sized room connecting to the Wireless and Networks Research Lab on level 1 of the University of Bristol's Merchant Venturers Building. This room had dimensions of 4 by 5 metres, a ceiling height

Antenna Pattern	Directivity (dBi)	Co-Polar Energy (%)	Cross-Polar Energy (%)	3 dB beamwidth
Antenna only	10.4	96.3	3.7	120°
On-body:				
Horizontal, Left	8.4	97.5	2.4	50°
Horizontal, Right	8.5	97.7	2.3	45°
Vertical, Left	7.8	97.9	2.0	60°
Vertical, Right	5.6	86.1	13.9	100°

TABLE I

ANTENNA CHARACTERISTICS, OFF- AND ON-BODY

TABLE II

SISO CHARACTERISTICS: CHANNEL ATTENUATION AND RICEAN K-FACTOR ESTIMATE

Antenna	1 - right side		2 - left side	
Distance	Att. (dB)	K-factor	Att. (dB)	K-factor
1 metre	30.5	23.8	39.9	5.9
2 metres	33.5	21.1	42.6	2.9
3 metres	38.2	15.6	37.3	7.7

of 3 metre, and has a suspended floor which consists of vinyl covered metal plates. The partitioning walls are made of plaster board in a metal frame and the outside wall consists of concrete and bricks. 80 cm below the reinforced concrete ceiling there is a framework with soft-boards that contains the lighting and hides several cables and pipes. During the measurements, the room was fairly empty, with some cardboard boxes on the lab benches and only a few chairs around. A diagram of the room and the measurement set-up can be found in figure 1.

B. Results

1) SISO channel characteristics: This section discusses the channel attenuation and fading characteristics of the SISO link. An analysis of MIMO characteristics, such as capacity and correlation between the spatial links, follows in the next section. Since only the vertically polarised channel data is considered for the MIMO schemes, the horizontally polarised links are not included in our discussions.

Table II presents the channel gain, in dB, and Ricean K-factor estimates, as a scalar, for the links between the on-body antennas and the linear array. The Ricean K-factor was estimated from the recorded frequency domain data using the method presented in [13]. The K-factor is used here as a measure for the dynamic range of the fading. It should be noted that this not imply that the fading is Ricean distributed.

Since the antennas at the uniform linear array have the same polarisation and orientation, the characteristics of the links to the individual array elements are similar. The characteristics have therefore been averaged over all elements at the receiving linear array.

Perhaps surprisingly, the difference in channel attenuation between the two on-body antennas is up to 10 dB. This highlights one of the problems with on-body antenna positioning: small variations in the position, alignment and orientation of the antennas on the body can lead to significant power imbalances, particularly when directional antennas are used. While the

link from the right antenna clearly has a high K-factor, more fading is present in the link from the left antenna, as indicated by the lower K-factor.

2) MIMO channel characteristics: In order to assess the potential of MIMO in LOS conditions, figure 2 compares the capacity of the SISO links with the capacity of a number of 2-by-2 MIMO systems. The transmitting end always consists of the vertical polarisations of the on-body antennas at the front of the user. At the receiving end, array element 1 is in turn combined with element 2 through to 8. The user stood 1 metre from the linear array facing towards it. A fixed transmit power was assumed; a value of 0 dBm is used as in Bluetooth. The noise floor was determined by the thermal noise in the 120 MHz bandwidth, together with a 10 dB noise figure, which produced a level of -80 dBm.

Despite the assumption that LOS results in highly correlated spatial sub-channels, and thus poor MIMO performance, figure 2 clearly shows that MIMO offers a significant capacity increase compared to SISO. In figure 3, it is first verified that the correlation between the measured subchannels is indeed high. The distributions of the magnitude of the complex correlation coefficients between the subchannels are shown grouped according to the element on the linear array that is combined together with element 1 to form the pair of receiving elements. Each curve consists of four sections, which correspond to the correlation between the paths arriving from or departing at the four antennas involved. It can be seen that in comparison with the IID Rayleigh reference channel, all the MIMO schemes suffer from highly correlated subchannels. The differences between the MIMO subchannels are minimal.

A possible explanation for the observed high MIMO capacity in LOS, despite the power imbalance (table II) and the high spatial correlation values, is provided by [14]. In this paper, Sakaguchi shows that, given a sufficiently high SNR, the channel capacity loss due to high spatial correlation is low. In the analysis, it is shown that, although high correlation leads to low eigenvalues, the high SNR ensures that all eigenmodes are activated.

From table II, it can be seen that with the chosen TX power and noise floor the signal-to-noise ratio on the sub-channels ranges from 30 to 50 dB. In order to investigate whether this high SNR is the cause of the MIMO capacity increases, the above capacity comparison was repeated for a fixed signal-to-noise ratio of only 10 dB. The results are shown in figure 4. For comparison, the capacity of an IID Rayleigh MIMO channel is also included.

At a fixed SNR of 10 dB, there is more variation in the capacity enhancements offered by MIMO compared to figure 2. Increasing the distance between the antennas on the linear array initially increases the capacity enhancement of MIMO. This reaches a maximum for array element 7, corresponding to an antenna spacing of 3.5λ, when the capacity of the resulting MIMO system outperforms the performance of the equivalent IID Rayleigh channel. Note that using array element 8 results in a drastic drop in the MIMO capacity.

Therefore, at least in some cases, the MIMO capacity increases observed in figure 2 are not solely due to the high signal-to-noise ratio. Even at a low signal-to-noise ratio, some of the channels approach, and even exceed, the capacity improvements seen in IID Rayleigh fading channels. Analysis of the eigenvalues, as shown in figure 5, reveals that the performance differences are also due to changes in the structure of the channel matrices.

In order to appreciate the origin of these differences, it is necessary to consider (1) the short distance between the transmitter and receiver, (2) the relatively large spacing between the antennas and (3) the LOS between the transmitter and receiver. At short ranges and/or with large antenna spacings, the spherical nature of the wave fronts can not be ignored [15]. It has been

TABLE III

MIMO ERGODIC CAPACITY IN BITS/S/HZ (FIXED SNR 20 DB, SISO: 6.7, IID RAYLEIGH: 11.6)

	Angle with ULA broadside		
Distance	0°	45°	90°
1 metre	11.8	10.3	10.7
2 metres	11.4	10.4	11.6
3 metres	12.0	10.1	11.7

shown that these spherical wave fronts can be exploited to achieve high capacity in LOS [15], [16], [17]. In pure LOS, the MIMO channel coefficients become deterministic. The phase difference between the channel coefficients is fixed and depends on the operating frequency, the array geometry and the array positions [16]. If the position of the antenna elements is such that orthogonal rows in the channel matrix are achieved, then the result will be a full-rank channel and maximum MIMO capacity will be achieved [16], [17] despite complete spatial correlation.

In the measurements, the phase relationship initially becomes closer to the optimum as the antenna spacing is increased. The combination of array elements 1 and 7 results in the best approximation. As demonstrated by elements 1 and 8, increasing the antenna spacing further will (initially) lead to a drop in capacity.

In figure 4, the drop in capacity when choosing one of the non-ideal elements is fairly significant. However, when assessing the practicality of this mechanism, it is necessary to keep in mind that the SNR was deliberately chosen to be very low, in order to minimise the effect of the mechanism described by Sakaguchi in [14]. In LOS PAN situations, however, a high SNR is to be expected. In that case, both mechanisms, [14] on the one hand and [16], [15] on the other, will be active and high capacity can be achieved despite non-ideal antenna placement. Using computer simulations, [18] had shown that significant capacity increases can be obtained over an area the size of a room (5 by 10 metres), even though the antenna spacings were calculated optimally for a 1 metre separation distance.

Here, the measurements are used to validate these predictions in a real-life scenario. Antenna elements 1 and 7 on the linear array were combined to form a 2-by-2 MIMO system with the on-body antennas. In addition to increasing the distance from the linear array, the user also stood at three different angles relative to the broadside of the linear array. Table III gives the ergodic capacity in the measured channels assuming the signal-to-noise ratio is fixed at 20 dB. As can be seen, the capacity remains close to the IID Rayleigh value, even when moving away from the array but still facing it. When standing perpendicular to the broadside of the array, the directional antennas require the link to utilise multipath propagation and the capacity is also close to IID Rayleigh. When standing at a 45 degree angle, the capacity increase compared to SISO is slightly lower, 53% instead of 73% for IID Rayleigh.

It is therefore concluded that MIMO can be used to enhance the throughput in a PAN. Although the presence of LOS leads to correlation, a high signal-to-noise ratio can compensate for this. Taking into account the short distances anticipated between PAN devices, these SNRs can be achieved with relatively low transmit powers (0 dBm in this analysis). Furthermore, it is possible to exploit the spatial correlation by placing the antennas further apart. Because of the deterministic nature of LOS links, this can lead to a phase relationship that results in an orthogonal channel matrix. Previous simulations [18], confirmed by these measurements, show that the capacity is not sensitive to deviations from orthogonality in the channel matrix and that

TABLE IV

USER ROUTINE DURING BAN MEASUREMENTS

duration	action
5 s	sitting down
5 s	standing up
5 s	marching on the spot
5 s	turning to the left and return to facing forward
5 s	turning to the right and return to facing forward
5 s	bending to touch the toes and return to standing

the system can lead to considerable capacity increase over a large area.

III. MIMO OPERATION IN A BAN

A. Measurement description

These measurement were conducted in co-operation with the author of [19]. A user was equipped with two arrays consisting of two dual-polar stacked patch antennas [12]. The antenna spacing is one wavelength. The on-body array locations are shown in figure 6. Inspired by [20], the user performed a 30 second routine as described in table IV. During this period, the channel responses were recorded in a 120 MHz bandwidth centred at 5.2 GHz using a Medav RUSK channel sounder [11].

The measurements were performed both in an empty office and in an anechoic chamber. The office is 6-by-7 m and 2.5 m high. The outer wall is made of bricks and concrete, while the walls along the corridor and between the offices are made of plasterboard on an aluminium frame. There is a wooden door that was kept closed during the measurements. The floor consists of metal sheets covered with floor tiles while soft boards cover the reinforced concrete ceiling. The window frames contain metal and a radiator is located underneath the large window. A diagram of the measurement location and set-up is shown in figure 7.

B. Results

1) SISO channel characteristics: As in [20], [21], evaluation of the SISO channel characteristics reveals the influence of the user and his actions. Obstruction of the LOS leads to significant body shadowing. The signal varies within a range of 45 and 25 dB in the anechoic chamber and the office environment respectively. Combined with user motion, body shadowing can lead to rapid changes in the channel. Figure 8 shows that the coherence time is reduced to tens of milliseconds during the dynamic phases of the measurement routine. Otherwise, the coherence time lies in the order of seconds, corresponding to the duration of the more static stages in the measurement.

Figure 9 shows the typical relationship between the channel attenuation and the RMS delay spread in the office environment. During periods of body shadowing, the link relies on multipath propagation present in the environment. Both the channel attenuation and the RMS delay spread are consequently high, while the Ricean K-factor is near zero. Low channel attenuation, indicative of the presence of a LOS, goes hand-in-hand with low RMS delay spreads and higher Ricean K-factors, up to 20.

Even during periods of low channel attenuation, the RMS delay spread is rarely zero. Three influencing factors have been identified: Firstly, the on-body location of the antennas means that they are oriented in an unpredictable, random manner. In

many cases, the antennas are not properly aligned: there is often a mismatch between polarisations at transmitter and receiver and the main beam of the antennas is not pointing in the optimal direction. Hence, the directionality and polarisation of the antennas can suppress the LOS component and thus increase the relative power of the multipath components. Secondly, the proximity of the body has been shown to lead to time dispersion of the perceived channel [22], [23]. Finally, spectral leakage will smear energy from the LOS components that fall between the centres of FFT bins. For the 1.25 MHz spacing of the recorded channel data, assuming the energy of a LOS component is equally spread between two neighbouring bins corresponds to an RMS delay spread of 4.2 ns.

2) MIMO channel characteristics: In this section, the recorded channels are combined to form MIMO channel matrices. The performance of both spatial and polarisation diversity based MIMO are analysed. In the measurements reported in [24], [25], MIMO based on polarisation diversity was shown to outperform single polarisation systems, especially in situations where the K-factor is high.

Using the capacity formula from [1], the results in figures 10 and 11 were calculated assuming a 2-by-2 MIMO system using the full 120 MHz measurement bandwidth.

Figure 10 assumes that the transmit power is fixed at 0 dBm. The noise floor was calculated as before and a value of -80 dBm was employed.

In order to demonstrate how capacity varies during the measurement routine, it is now plotted against time for one of the antenna configurations for the links from chest to wrist. As was the case for the SISO links, the user movements influence the characteristics of the MIMO link. Not only does the user motion lead to changes in the channel matrix coefficients, but this is also combined with power variations due to body shadowing. The net result is a significant variation in the capacities of the MIMO systems. The distribution for all possible combinations of antennas in all the measurements shows that whereas the SISO capacity ranges from 2 to 10 bits/s/Hz, the MIMO capacity varies from 4 to 20 bits/s/Hz.

Figure 11, presents a similar analysis but with the signal-to-noise ratio fixed at 20 dB. This corresponds to a system with ideal and unlimited power control. Since such system removes the influence of power variations in the capacity results, it allows us to investigate the influence of changes in the channel matrix structure on capacity. These changes are isolated from the influence of differences in the received signal strength. Figure 10 demonstrates that the MIMO capacities observed are not solely due to high SNR [14].

For comparison, the capacity of an equivalent system operating in an IID Rayleigh fading channel is also included. For the plot showing evolution during the measurement routine, the ergodic capacity of the IID Rayleigh fading channels is shown. Both the spatial and polarisation diversity schemes lead to significant capacity increases. Looking at the capacity distribution from all measurements, the ergodic capacity of the spatial diversity scheme is slightly less than that of the IID Rayleigh reference, while the ergodic capacity of the polarisation diversity scheme is slightly higher. The 10% outage capacity is slightly lower than the IID Rayleigh reference in the case of polarisation diversity and markedly lower for the spatial diversity scheme.

The difference between the efficiency of the polarisation and spatial diversity schemes is reflected in the eigenvalue structure of their respective channel matrices. In the case of polarisation diversity, the eigenvalues are closer to the ideal case where they have equal powers. Figures 13 and 14 show that, although the power ratio between the entries in the channel matrix is slightly better using the spatial diversity scheme, this advantage is cancelled by the fact that they are also more correlated.

IV. Conclusions

In this paper, the use of MIMO in the personal sphere has been examined. Analysis of a first measurement campaign, where a user equipped with two on-body antennas stood in front of a linear array, has shown that even under LOS conditions, MIMO can be used in PAN applications. Correlation between the links can be overcome by high signal power and/or the deterministic nature of the LOS links. This latter mechanism allows us to approximate an orthogonal channel matrix by placing the antennas further apart. Due to the logarithmic relationship between the channel matrix product and the capacity, deviations from the optimal antenna placement can still result in a significant MIMO capacity increase, which was shown using the measured channel data.

The use of MIMO in body area networks was examined in a second measurement campaign. User actions combined with body shadowing were shown to lead to rapid changes in the channel. During the dynamic periods of the measurement routine, the coherence time was reduced to tens of milliseconds. Analysis of the MIMO capacity focussed on the relative merits of spatial and polarisation diversity. Although the latter suffers from a more unfavourable power imbalance, the links were also less correlated, leading to a better performance when fixed SNR is assumed. Power variations due to body shadowing were seen to lead to significant variations in the capacity of the MIMO link.

Acknowledgments

Part of this work was funded by the Core 3 Research Programme of the Virtual Centre of Excellence in Personal and Mobile Communications, Mobile VCE, (www.mobilevce.com), whose funding support, including that of EPSRC, is gratefully acknowledged. The authors also would like to thank Richard Smerin for his involvement in recording the BAN channels.

References

[1] Foschini, G.J., and Gans, M.J.: 'On Limits of Wireless Communications in a Fading Environment when Using Multiple Antennas' Wireless Pers. Commun., 1998, 6, pp. 331–335

[2] Foo, S.E.: 'Spatial Temporal Characterisation of UTRA FDD Channels at the Base Station and Mobile Terminal'. PhD thesis, University of Bristol, 2004

[3] Kermoal, J.P.: 'Measurement, Modelling and Performance Evaluation of the MIMO Radio Channel'. PhD thesis, Aalborg University, 2002

[4] McNamara, D.P.: 'Characterisation and Investigation of Multiple-Input Multiple-Output Wireless Communication Channels'. PhD thesis, University of Bristol, 2003

[5] Shiu, D.S., Foschini, G.J., Gans, M.J., and Kahn, J.M.: 'Fading Correlation and Its Effect on the Capacity of Multielement Antenna Systems', IEEE Trans. Commun., 2000, 48, (3), pp. 502–513

[6] Chuah, C.N., Tse, D.N.C., Kahn, J.M., and Valenzuela, R.A.: 'Capacity scaling in MIMO wireless systems under correlated fading', IEEE Trans. Inform. Theory., 2002, 48, (3), pp. 637–650

[7] 'Bluetooth™v1.1 Foundation Specifications', 1999

[8] 'Specifications of the Bluetooth System, v2.0', 2004

[9] 'IEEE 802.15 Working Group for Wireless Personal Area Networks (WPANs)', www.ieee802.org/15/

[10] Johansson, A., Karedal, J., Tufvesson, F., and Molisch, A.F.: 'MIMO Channel Measurement for Personal Area Networks', VTC 2005-Spring. vol. 1, 2005, pp. 171–176

[11] Thoma, R.S., Hampicke, D., Richter, A., Sommerkorn, G., Schneider, A., Trautwein, U., et al.: 'Identification of Time-Variant Directional Mobile Radio Channels', IEEE Trans. Instrum. Meas., 2000, 49, (2), pp. 357–364

[12] Paul, D.L., Craddock, I.J., Railton, C.J., Fletcher, P.N., and Dean, M.: 'FDTD analysis and design of probe-fed dual-polarized circular stacked patch antenna', Microw. Opt. Techn. Let., 2001, 29, (4), pp. 223–226

[13] Greenstein, L.J., Michelson, D.G., and Erceg, V.: 'Moment-method estimation of the Ricean K-factor', IEEE Commun. Lett., 1999, 3, (6), pp. 175–176

[14] Sakaguchi, K., Chua, H.Y.E., and Araki, K.: 'MIMO Channel Capacity in an Indoor Line-Of-Sight (LOS) Environment', IEICE Trans. Commun., 2005, E88-B, (7), pp. 3010–3019

[15] Jiang, J.S., and Ingram, M.A.: 'Distributed source model for short-range MIMO', VTC 2003-Fall. vol. 1, 2003, pp. 357–362

[16] Driessen, P.F., and Foschini, G.J.: 'On the Capacity Formula for Multiple Input - Multiple Output Wireless Channels: A Geometric Interpretation', IEEE Trans Commun. 1999, 47, (2), pp. 173–176

[17] Sarris, I., and Nix, A.: 'Design and performance assessment of maximum capacity MIMO architectures in line-of-sight', IEE Proc. Commun., 2006, 153, (4), pp. 482 – 488

[18] Neirynck, D., Williams, C., Nix, A., and Beach, M.: 'Personal Area Networks with Line of Sight MIMO Operation', VTC 2006-Spring. Melbourne, Australia, 2006

[19] Smerin, R.: 'Channel Modelling for Body Area Networks'. MEng. Dissertation, University of Bristol, 2005

[20] Hall, P.S, Ricci, M., and Hee, T.M.: 'Measurements of on-body propagation characteristics', IEEE Antennas Propagat. Soc. Int. Symp., vol. 2, 2002. pp. 310–313

[21] Neirynck, D., Williams, C., Nix, A., and Beach, M.: 'Wideband Channel Characterisation for Body and Personal Area Networks', Int. Workshop on Wearable and Implantable Body Sensor Networks, London, United Kingdom, April 2004

[22] Sanchez, M.G., de Haro, L., Pino, A.G., and Calvo, M.: 'Human operator effect on wide-band radio channel characteristics' IEEE Trans. Antennas Propagat., 1997, 45, (8), pp. 1318–1320

[23] Pinkney, J., and Sesay, A.: 'Characterization of the on-body wireless channel at 2.4 and 5.8 GHz', VTC-2005-Fall. vol. 2, 2005. pp. 1294–1298

[24] Kyritsi, P., Cox, D.C., Valenzuela, R.A., and Wolniansky, P.W.: 'Effect of antenna polarization on the capacity of a multiple element system in an indoor environment', IEEE J. Select. Areas Commun., 2002, 20, (6), pp. 1227–1239

[25] Erceg, V., Sampath, H., and Catreux-Erceg, S.: 'Dual-Polarization Versus Single-Polarization MIMO Channel Measurement Results and Modeling', IEEE Trans. Wireless Commun., 2006, 5, (1), pp. 28–33

LIST OF FIGURES

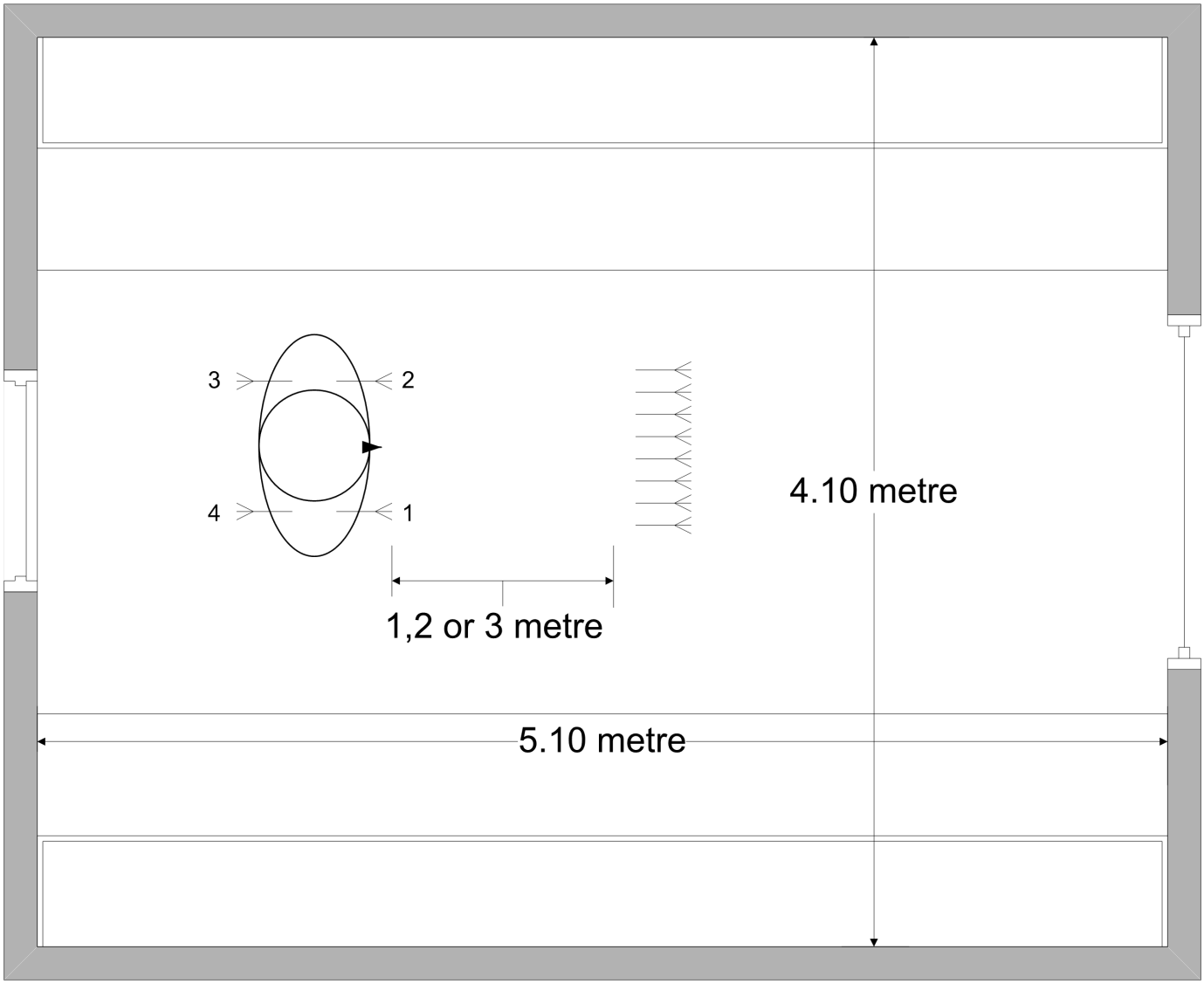

Fig. 1. Measurement location and set-up for the PAN measurements

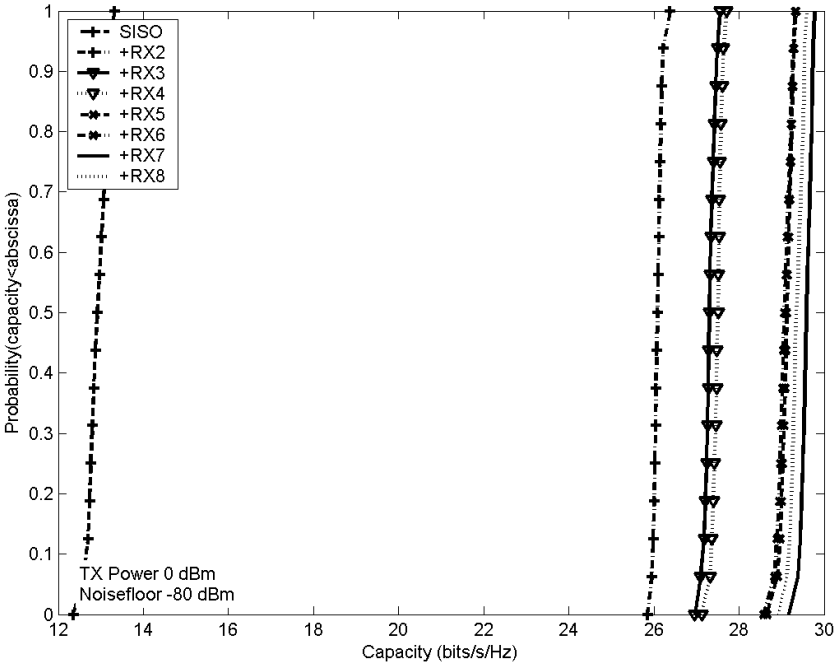

Fig. 2. Capacity comparison using a fixed transmit power and noise floor

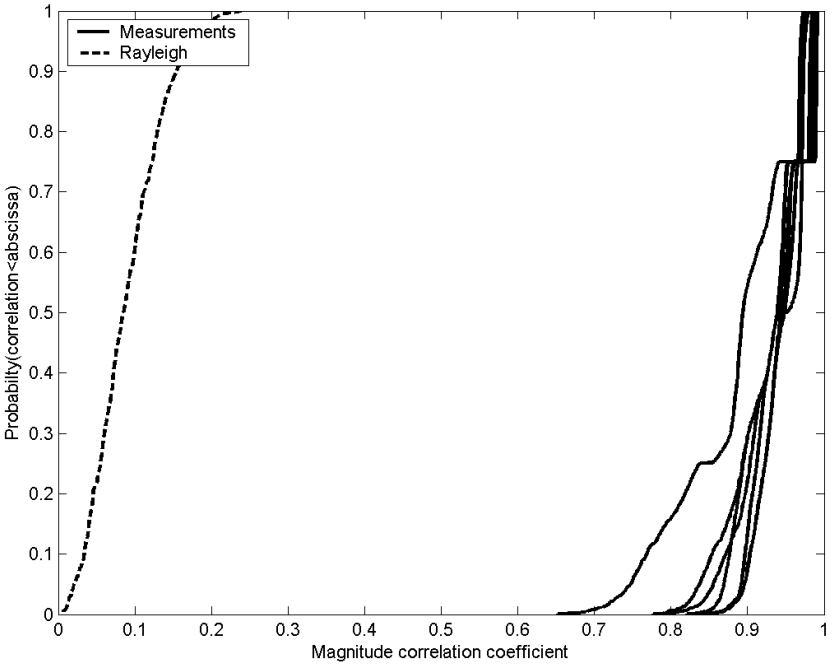

Fig. 3. Comparison magnitude correlation coefficient distributions

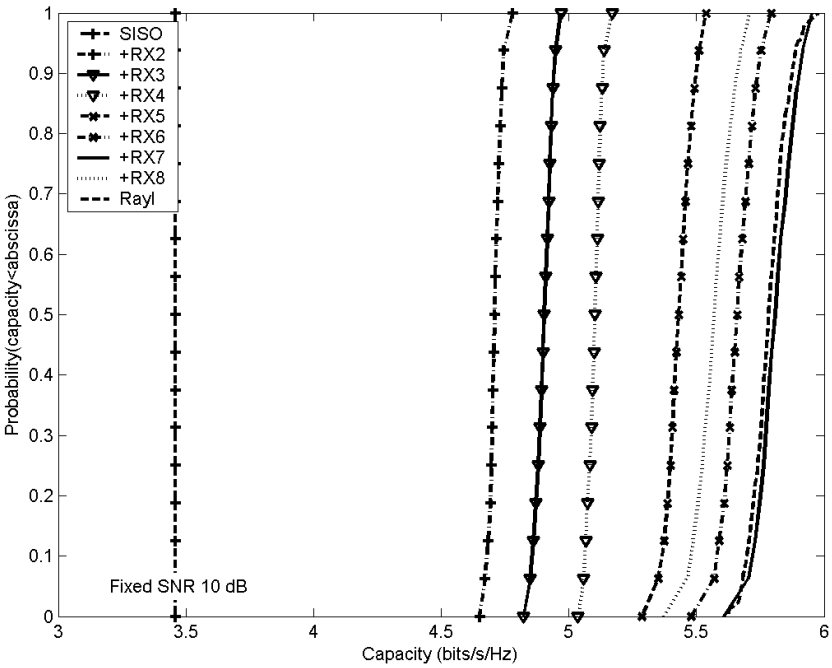

Fig. 4. Capacity comparison using fixed SNR

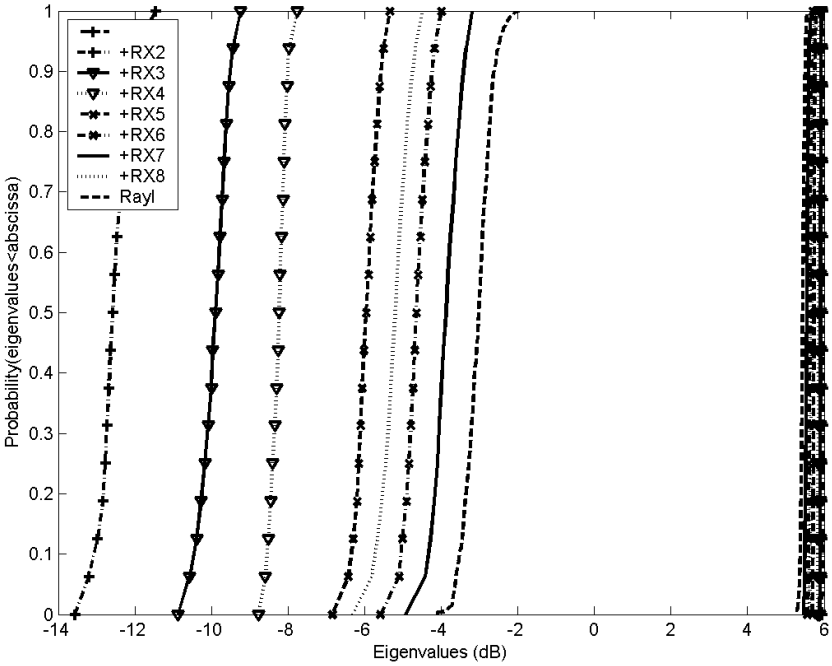

Fig. 5. Comparison Eigenvalue distributions

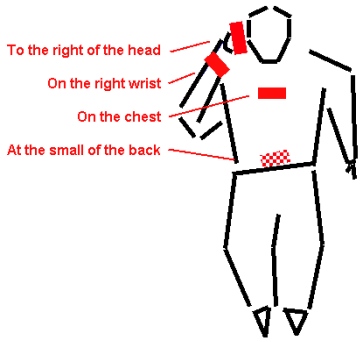

Fig. 6. Array locations in the BAN measurement

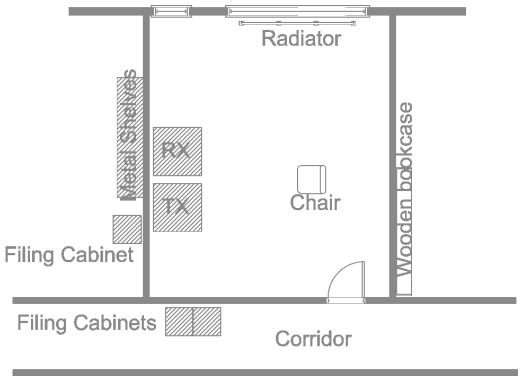

Fig. 7. Measurement set-up for the BAN measurement

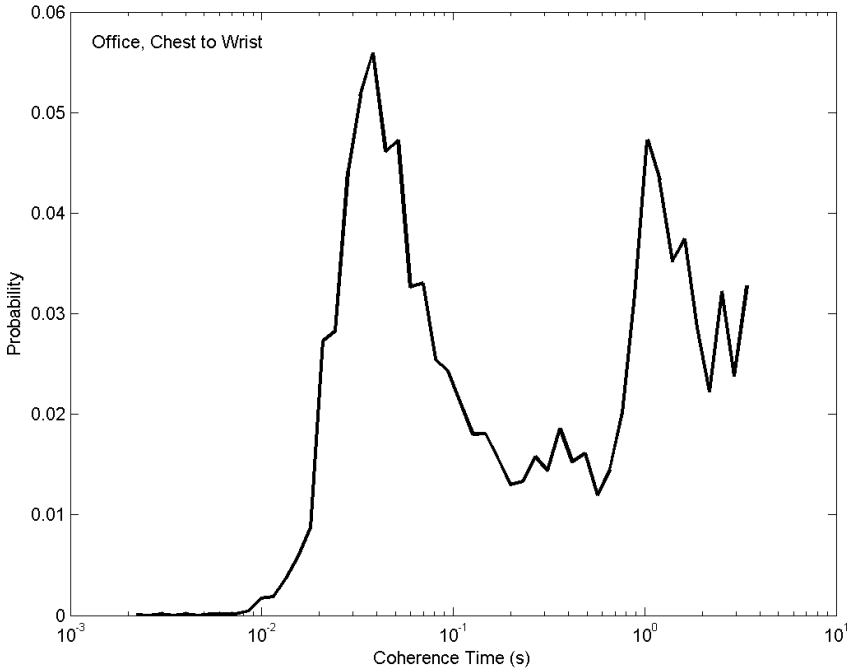

Fig. 8. Distribution of coherence time during the measurement routine

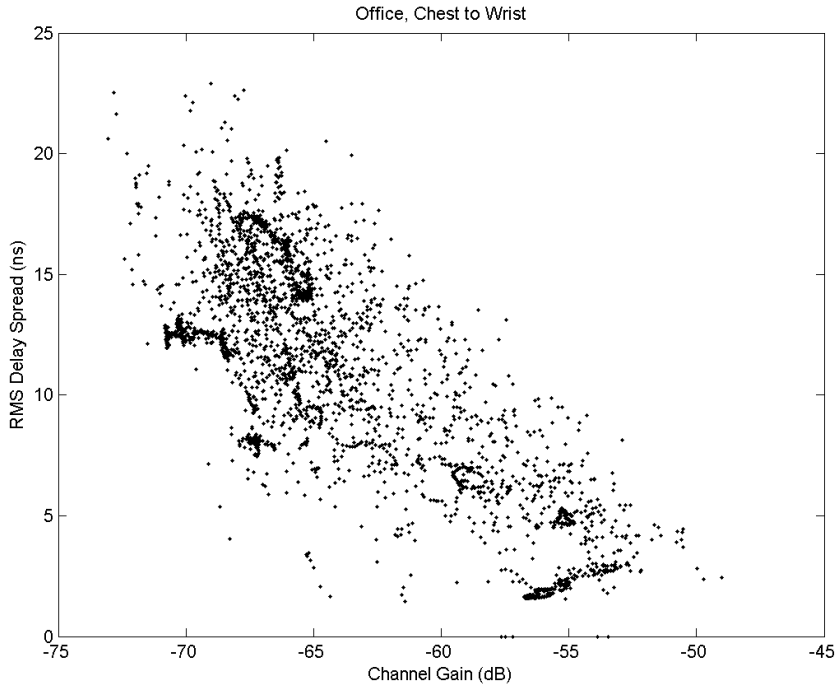

Fig. 9. Scatterplot of channel gain versus RMS delay spread

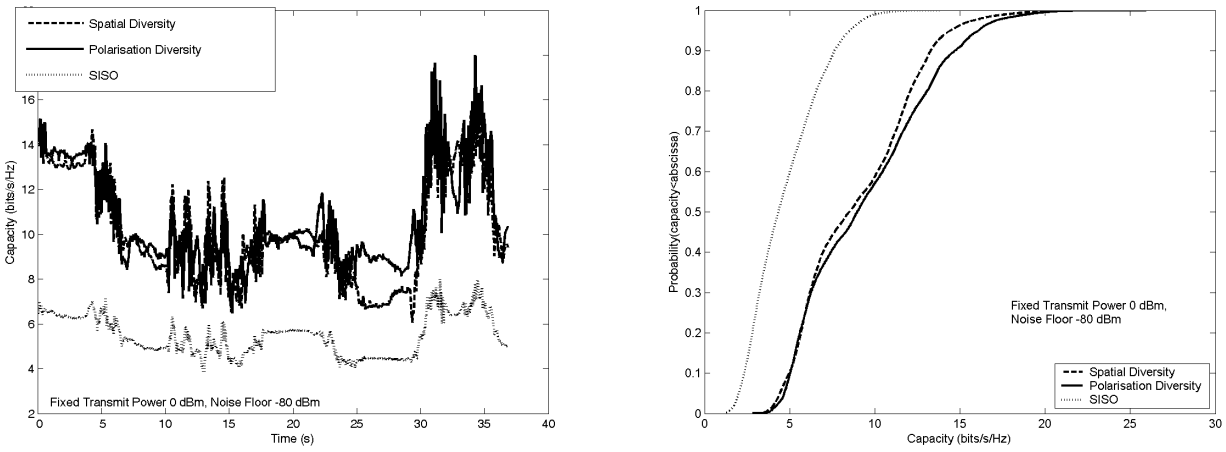

(a) Evolution chest-to-wrist link

(b) Distribution over all office measurements

Fig. 10. Capacity in on-body measurements when using fixed TX power and noise floor

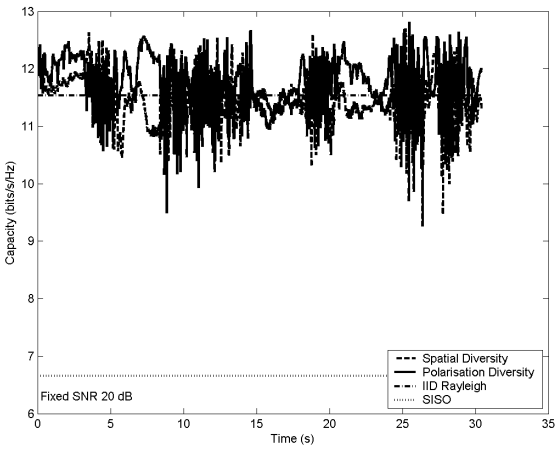

(a) Evolution chest-to-wrist link

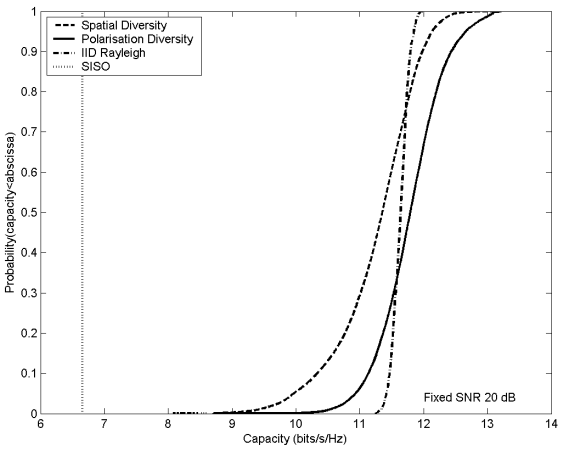

(b) Distribution over all office measurements

Fig. 11. Capacity in on-body measurements when using fixed SNR

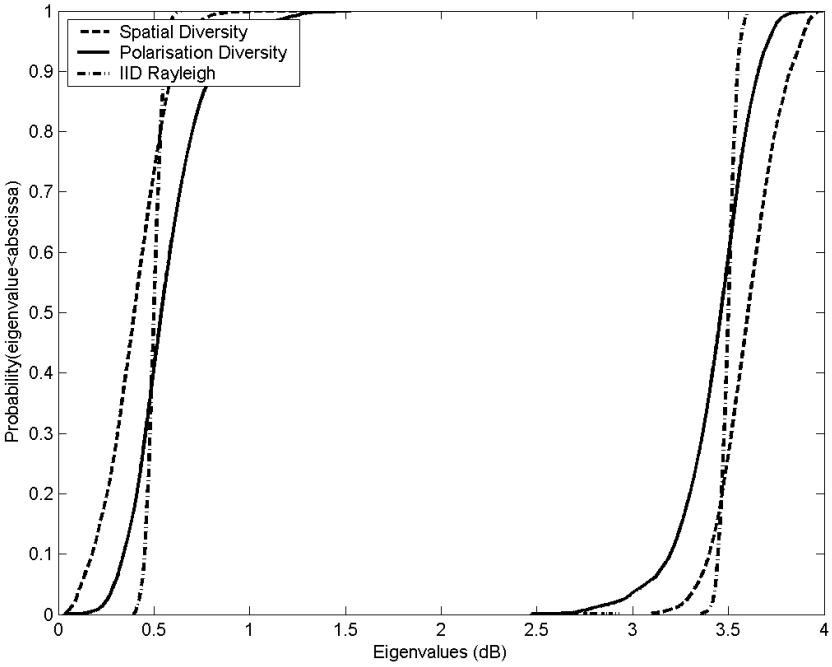

Fig. 12. Distribution of Eigenvalues in all on-body measurements

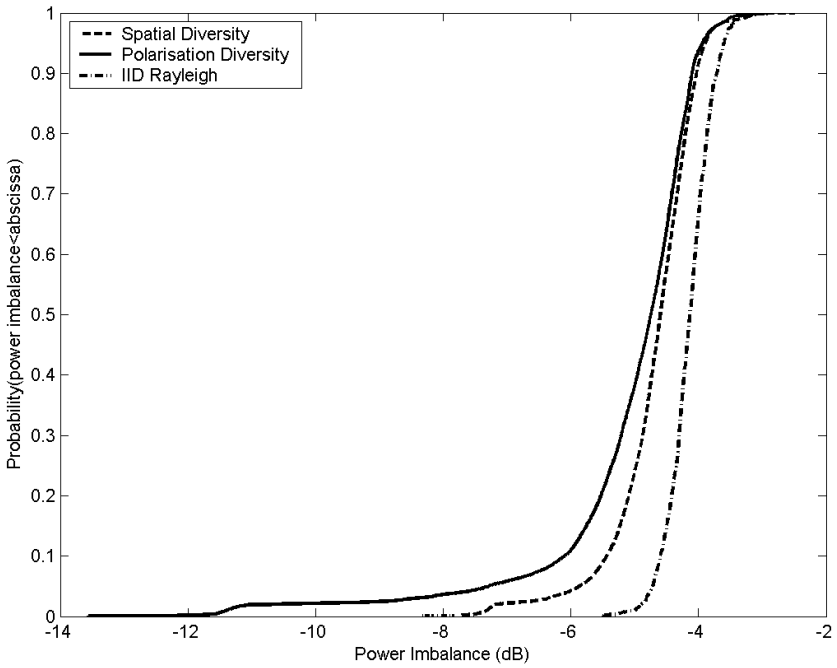

Fig. 13. Distribution of branch power ratios in all on-body measurements

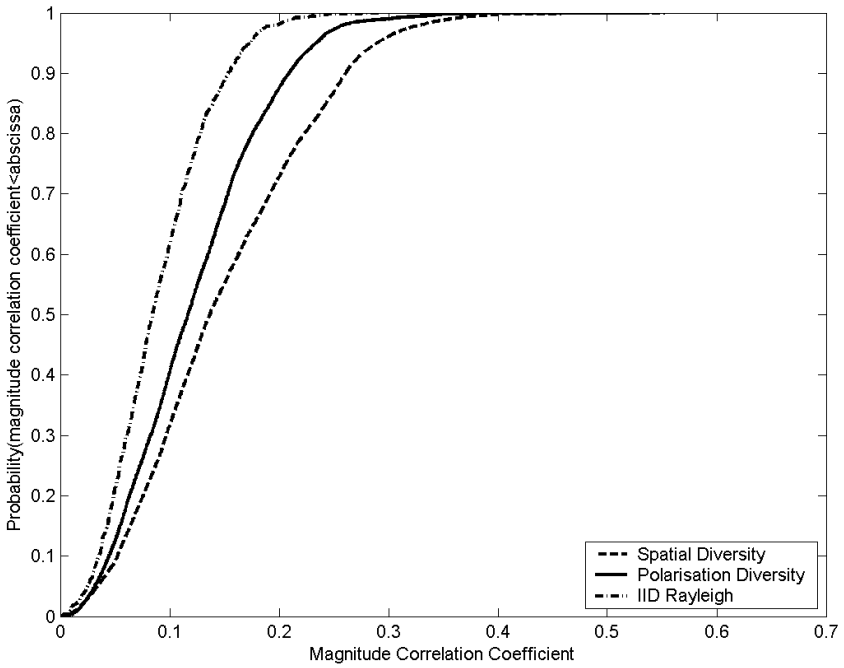

Fig. 14. Distribution magnitude of correlation coefficient in all on-body measurements